This article has been accepted for publication in IEEE Access. This is the author's version which has not been fully edited and content may change prior to final publication. Citation information: DOI 10.1109/ACCESS.2025.3572554

IEEE Access
Multidisciplinary | Rapid Review | Open Access Journal

Date of publication xxxx 00, 2025, date of current version xxxx 00, 2025.

Digital Object Identifier xxx/ACCESS.2025.DOI

Enhanced ANN-Based MPPT for Photovoltaic Systems: Integrating Metaheuristic and Analytical Algorithms for Optimal Performance Under Partial Shading

ALPASLAN DEMIRCI[1], IDRISS DAGAL[2], SAID MIRZA TERCAN[1], HASAN GUNDOGDU[1], MUSA TERKES[1] and UMIT CALI[3,4] (Senior Member, IEEE)

[1]Department of Electrical Engineering, Yildiz Technical University, 34220 Istanbul, Türkiye
[2]Department of Electrical-Electronics Engineering, Istanbul Beykent University, 34396 Istanbul, Türkiye
[3]Department of Electric Power Engineering, Norwegian University of Science and Technology, 7034 Trondheim, Norway
[4]School of Physics, Engineering and Technology, University of York, YO10 5DD York, United Kingdom

Corresponding author: Umit Cali (e-mail: umit.cali@ntnu.no).

ABSTRACT The efficiency of photovoltaic (PV) systems significantly decreases under partial shading conditions (PSC), leading to challenges in accurately tracking the maximum power point (MPP). This paper presents an enhanced Artificial Neural Network (ANN) to improve the performance of MPP tracking (MPPT) in PV systems subject to PSC. The proposed algorithm is based on an advanced ANN model trained with widely known analytical and metaheuristic algorithms, providing higher accuracy and faster convergence than existing methods. Furthermore, the ANN model was developed and trained using an extensive dataset that includes diverse shading scenarios, irradiation levels, and temperature conditions, with metaheuristic algorithms playing a key role in enhancing its training process. The performance of the proposed system has been evaluated through extensive simulations and sensitivity analyses. The results demonstrate that the improved ANN-based MPPT algorithm consistently outperforms existing MPPT techniques, including the Perturb and Observe (P&O) and Grey Wolf Optimization (GWO), Harris Hawks Optimization (HHO), and Particle Swarm Optimization (PSO) methods. The proposed approach achieves higher efficiency, faster response times, and improved stability under dynamic shading conditions. Specifically, its superior efficiency reaches up to 99.98% under constant shading conditions (CSC) and up to 99.97% under PSC, as verified through extensive simulations using MPPT efficiency metrics. This advancement holds significant potential for optimizing the energy yield of PV systems, promoting more reliable and efficient renewable energy solutions, especially when operating in challenging environmental conditions.

INDEX TERMS Artificial neural network, Maximum power point tracking, Metaheuristic algorithms, Partial shading, Photovoltaic

I. INTRODUCTION

In recent years, renewable energies extracted from solar and wind sources have emerged as ideal solutions for fulfilling energy needs, offering significant benefits such as minimal environmental impact and the ability to supply energy sustainably without limitations. Traditional power systems are progressively evolving into microgrids that integrate localized and autonomous renewable energy sources (RESs) for both generation and distribution of power [1]. The optimal operation of RES-based microgrids presents a significant challenge due to their inherent nonlinear characteristics and the high penetration levels of distributed RES units. The role of Maximum Power Point Tracking (MPPT) in ensuring the smooth and uninterrupted operation of standalone DC microgrids, particularly under varying penetration levels of RESs, has gained significant attention in recent literature.

This work is licensed under a Creative Commons Attribution-NonCommercial-NoDerivatives 4.0 License.
For more information, see https://creativecommons.org/licenses/by-nc-nd/4.0/

This article has been accepted for publication in IEEE Access. This is the author's version which has not been fully edited and
content may change prior to final publication. Citation information: DOI 10.1109/ACCESS.2025.3572554

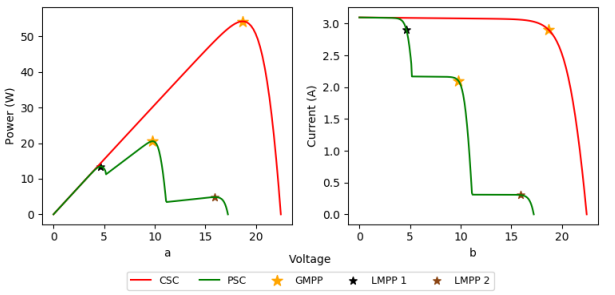


FIGURE 1. Maximum power points on the P-V

MPPT is crucial for optimizing energy generation from photovoltaic (PV) systems, especially in scenarios where RES penetration fluctuates, leading to intermittent energy supply. Under high penetration of RESs, the variability of renewable generation can cause voltage and frequency instabilities within the microgrid. Therefore, MPPT techniques are essential for dynamically adjusting the energy output of PV systems to match load demand, ensuring that energy generation remains continuous and efficient. Furthermore, in instances of minimal RES integration, the integration of ancillary energy sources such as batteries or diesel generators assumes paramount importance. MPPT, when combined with intelligent energy management systems, can also help direct excess energy to dump loads, preventing overcharging of storage systems and maintaining system stability [2]. This combination of strategies ensures that the standalone microgrid operates smoothly, even under fluctuating energy availability [3]. This study examines solar PV systems, which are widely appreciated for their ease of installation, by evaluating their performance under both clear sky conditions (CSC) and partial shading conditions (PSC). Environmental factors such as shading can significantly reduce the energy production of PV panels, affecting their overall efficiency. To mitigate this issue, an enhanced artificial neural network (ANN) is proposed for MPPT, aimed at optimizing energy generation under varying shading conditions. The relationship between the maximum power points (MPP) and PV power and voltage, as illustrated in Figure 1, underscores the effectiveness of this approach in optimizing PV system performance.

Numerous studies have been performed to track global MPP under several PSCs using various metaheuristic optimization algorithms. These methods have been tried to significantly reduce tracking time, power losses, and oscillations, enhancing efficiency [4]. It is required that they avoid falling into a local maximum, especially under PSC, and can easily be implemented. Particle Swarm Optimization (PSO) is a bio-inspired, intelligence-based metaheuristic optimization algorithm. The PSO technique performs better than the conventional MPPT methods, which cannot track global MPP (GMPP) under PSC [5]. PSO has been extensively used for various engineering applications due to good accuracy, simpler structure, high adaptability, and few tuning parameters. Still, it has drawbacks like steady-state oscillation, convergence ability, and tracking speed. Therefore, improving PSO regarding searching speed and reducing oscillation has gained enormous attention from researchers [6]. Harris Hawks optimization (HHO) has been applied recently for several engineering problems, like an MPPT algorithm to find the global MPP of PV array during PSC [7, 8]. The advantages of HHO for MPPT are effectively minimizing the undesired steady-state oscillation and high-power conversion efficiency with reasonable accuracy. However, HHO may fall into local maximum points, and finding the MPP under PSC takes longer. Grey Wolf Optimization (GWO), a bio-inspired swarm-based metaheuristic algorithm, gives competitive results compared to popular swarm-based algorithms regarding accuracy, convergence independency, simple control, and the ability to deal with local minima [9]. After GWO's first use as MPPT [10], an enhanced version of GWO was also used as GMPPT for the PV system under PSC, simplifying the calculation process with high accuracy [11]. In addition to widely used and well-established algorithms such as PSO, HHO, and GWO, the Black Widow Optimization (BWO) has recently attracted attention due to its robust convergence characteristics and strong ability to avoid local optima, as demonstrated in recent microgrid energy management studies. The BWO-based control strategy provides fast convergence, enhanced global search capability, and low computational complexity, making it a promising candidate for MPPT applications under complex and dynamically changing shading conditions. [12]

The stated issues encourage hybridizing metaheuristic algorithms to get better tracking speed results and avoid falling into local maxima. For example, Genetic Algorithm (GA) and PSO are the most popular methods. GA has an inconvenience in the converging rate, and PSO may get stuck in local extremes. A hybrid PSO-GA is presented to suppress these weaknesses [22]. In recent decades, multi-layer perceptron ANN has emerged as a leading machine learning technique, particularly in the field of solar energy. Furthermore, given that the most crucial phase of ANN training is optimization, researchers have focused their attention on this theory to address a significant challenge associated with ANN: its tendency to become trapped in local minima. Consequently, numerous researchers have endeavored to employ diverse optimization algorithms to enhance ANN performance. Examples of such algorithms include PSO, GA, Imperialist Competitive Algorithm (ICA), and Ant Colony Optimization (ACO) techniques [23]. In recent years, the ANN method has garnered significant interest from researchers in the field of nonlinear system prediction, mainly due to its robust simulation capabilities. The ANN is constituted of numerous neuron elements, which are positioned in the network's distinct layers. The primary layers of the multi-layer perceptron neural network are the input, hidden, and output layers, as illustrated in Figure 9. ANN is composed of neurons and their internal linkages, with the transmitted signal multiplied by a weight for each of these components. One of the main

This work is licensed under a Creative Commons Attribution-NonCommercial-NoDerivatives 4.0 License.
For more information, see https://creativecommons.org/licenses/by-nc-nd/4.0/

This article has been accepted for publication in IEEE Access. This is the author's version which has not been fully edited and
content may change prior to final publication. Citation information: DOI 10.1109/ACCESS.2025.3572554

TABLE 1. Comparative Analysis of Advanced MPPT Techniques

Reference	Technique	Summary
[13]	Projectile Search Algorithm (PSA)	PSA simulates projectile motion for MPPT, outperforming PSO, Jaya, and Cuckoo Search. Achieves 99.06% efficiency with 1.5s convergence to the GMPP, superior stability, and minimal oscillations, making it ideal for dynamic conditions.
[14]	Hybrid PSO (HPSO)	HPSO outperforms ACO, GWO, CS, P&O, and PSO under PSCs. Achieves a 27% efficiency increase and faster convergence, reducing search space and oscillations. HPSO is suitable for low-cost microcontrollers with 20-22% improvement in tracking efficiency.
[15]	GWO-Enhanced PSO for MPPT	Combines GWO and PSO to optimize MPPT performance under challenging conditions. Increases energy production by 21.62%, offering faster response times and higher efficiency compared to P&O and PSO.
[2]	Search and Rescue Algorithm (SRA)	Introduces an SRA-based MPPT for PV systems under complex and composite PSC. The SRA outperforms PSO, GWO, CS, GHO, and PSO-(GS), offering 8% more power, 5% more energy, and faster convergence (180% improvement). Real-world data shows 99.93% tracking efficiency.
[16]	Improved Grey Wolf Optimization (IGWO)	Proposes IGWO for faster tracking and higher efficiency (82% faster convergence, 2.3% more energy). The method narrows the search space and avoids local maxima, improving runtime by 76%. Validated under dynamic weather conditions, outperforming P&O, PSO, HHO, and GWO.
[17]	Improved Salp Swarm Algorithm (ISSA)	Enhances SSA for faster convergence and accuracy in PSC. Uses chaotic initialization and dynamics inspired by Levy flight and lion swarm. Outperforms P&O, SSA, and PSO with fastest convergence and highest accuracy in simulations.
[18]	ANN-Adaptable Supported Stepped-Scaled P&O (ANN-ASSPO)	Introduces an ANN-supported hybrid MPPT technique for interleaved boost converters. Provides fast and stable tracking, with efficiency up to 99.80%, and reduced settling time (2.06 s) compared to Water Cycle Optimisation-P&O. Low computational complexity, practical for real applications.
[19]	Metaheuristically Modified ANN-MPPT (HHO, GWO, PSO)	Enhances ANN-MPPT with metaheuristic optimization (HHO, GWO, PSO), improving performance under varying irradiance. HHO-based ANN-MPPT shows superior performance with lower computational time and higher efficiency, especially under shading.
[20]	ANN-Based MPPT Control of Modified Flyback Converter	Proposes ANN-based MPPT for a modified flyback converter, using MOSFET for efficiency and reduced voltage stress. Shows better dynamic response and system longevity with up to 90.2% efficiency compared to P&O-PSO controllers.
[21]	ANN-Based GMPPT	A global maximum power point tracking (GMPPT) method using ANN without the need for irradiance or temperature sensors. Achieves excellent performance with tracking time of 0.18s, power loss of 0.01W, and 99.66% accuracy. Suitable for low-cost DSC applications.
This Study	Enhanced ANN-based MPPT for PV Systems	Proposes a hybrid-trained ANN MPPT achieving 99.97% efficiency under PSC with 0.092s convergence time, offering improved accuracy and adaptability over conventional and heuristic algorithms.

differences between the performance of ANNs lies in the size of the hidden layers and their neurons. In other words, an essential step in training the ANN model is to determine the number of hidden layers and their neurons. The network should be trained with an adequate pair of input-output data using an optimization algorithm [24]. Table 1 provides a comparative overview of recent MPPT algorithms developed for PV systems, particularly under PSC. The table highlights the main features of the algorithms, the tracking efficiency gains, the convergence time and the practical applicability of the algorithms. This analysis allows the identification of the most suitable algorithms for dynamic and complex environmental conditions.

Researchers have also applied ANN as MPP controllers to track the solar PV module's global maximum power point [25]. ANN is commonly recognized as a new approach to solving complicated problems and has been immensely used in various fields. ANN-based MPPT real-time controller has been used to announce the grid-connected solar PV power systems [26]. The ANN works based on the "black-box" model [27]. The neuron is the most prominent processing element of an ANN. The ANN extracts the required information directly from the data that diverged from conventional techniques. The ANN methods are trained to solve complex problems challenging human beings and computer memories. A type of neuron named biological neuron gets the inputs from other suppliers, blending them in some ways by applying the nonlinear operation on the result to achieve

This work is licensed under a Creative Commons Attribution-NonCommercial-NoDerivatives 4.0 License.
For more information, see https://creativecommons.org/licenses/by-nc-nd/4.0/

This article has been accepted for publication in IEEE Access. This is the author's version which has not been fully edited and
content may change prior to final publication. Citation information: DOI 10.1109/ACCESS.2025.3572554

the result. In current MPPT application studies, bio-inspired algorithms like PSO, ACO, and GA impressively attracted the attention of researchers due to the satisfactory accuracy when treating stochastic, nonlinear, and undifferentiable optimization issues without considering more mathematical computations [28, 29]. Moreover, they present numerous feature advantages such as different simplicity of implementation, easy calculation, and swift response. This study proposes an enhanced ANN, integrating analytical and metaheuristic techniques to improve tracking accuracy and convergence speed over traditional methods. The ANN model is trained using a comprehensive dataset that includes various shading scenarios, irradiation levels, and temperature conditions. The original contributions of this paper are as follows:

- An advanced ANN-based MPPT algorithm is introduced to significantly boost the efficiency of PV systems under partial shading conditions.
- The algorithm, trained with analytical and metaheuristic methods, provides higher accuracy and faster convergence compared to existing methods.
- The results confirm that the ANN-based MPPT approach offers superior tracking accuracy and faster response times compared to existing algorithms under various shading conditions.
- The results highlight that the proposed system outperforms existing MPPT techniques, achieving up to 99.98% efficiency under constant shading and 99.97% under partial shading.

This article is organized as follows. Section I introduces the literature review and contributions. Section II describes the methodology, mathematical modeling, and problem statement. Section IV compares and evaluates the results. Finally, Section V concludes and provides recommendations for future work.

II. METHODOLOGY

The following sections explain the methodology for improving the performance of the ANN-based MPPT algorithm under PSC.

A. PROBLEM STATEMENT

The pursuit of efficient and reliable MPPT in PV systems has prompted substantial research into various algorithms designed to enhance energy capture. The conventional MPPT techniques encompass a range of methodologies, including metaheuristic approaches such as GA and PSO, as well as analytical methods such as P&O and Incremental Conductivity (IC). Even though these approaches have shown to be effective, they still come with certain limitations.

Although robust and flexible, metaheuristics often require extensive computational resources and can be susceptible to convergence issues, which may result in sub-optimal performance in rapidly changing environments. In contrast, analytical methods, which are often simpler and faster, can suffer from reduced accuracy and stability, especially in dynamic and irregular operating conditions. These methods may fail to adequately respond to the complex, nonlinear, and time-varying nature of PV systems, which may affect the overall efficiency and reliability of the energy extraction process.

In contrast, ANNs present a promising alternative due to their capacity to model intricate, nonlinear relationships and adapt to evolving circumstances through learning and optimization. ANN can process historical and real-time data to predict and monitor the MPP with a high degree of accuracy, which has the potential to exceed the performance of traditional methods. This adaptive capability enables ANN to handle various operating scenarios and uncertainties more effectively, which may result in improved energy efficiency and system reliability. ANN can learn and predict MPPT behaviors dynamically using historical and real-time data, whereas metaheuristic algorithms rely on search-based methods. Unlike fixed-rule algorithms like GWO and HHO, ANN can adapt its parameters with continued learning, improving its performance over time. ANN can continuously learn from changing environmental conditions (e.g., shading and irradiance patterns), making it highly effective for dynamic MPPT scenarios. By modeling and predicting the PV array's power characteristics, ANN reduces tracking time and energy losses. ANN can be integrated with existing optimization algorithms to form hybrid solutions, leveraging its predictive accuracy with the optimization capability of methods like GWO or HHO [16].

This paper examines why ANN is a more practical approach than traditional metaheuristic and analytical methods for MPPT detection. By reviewing each method's relative merits and limitations and elucidating the distinctive advantages of ANN-based techniques, we seek to demonstrate how ANN can address the shortcomings of existing MPPT strategies and enhance the performance of PV systems.

B. PROPOSED METHOD

First, PV models for CSC and PSC were designed, then shading patterns were introduced, and finally, PV characteristics were generated.

- **Designing PV Models**

In Figure 2, the circuit diagram consists of the 3SP2 solar panel connection, the buck converter, the proposed ANN, and other algorithms. In the block diagram, the PSC model is formed by the different irradiances, and the CSC series-connected panels work under the same irradiance.

DC/DC buck converter was designed using the PySpice library [30] in the Python environment. The parameters are given in Table 2. In this study, the converter's operating frequency is 20 kHz.

PV model (PVM) simulates characteristic curves of PV arrays in any weather conditions. Numerous PVMs are based on the equivalent circuits of single-diode and two-diode [31–34]. Additionally, PVMs based on a three-diode equivalent circuit better show the losses, but it is quite complex due to nine unknown parameters. PVM parameters are determined

This work is licensed under a Creative Commons Attribution-NonCommercial-NoDerivatives 4.0 License.
For more information, see https://creativecommons.org/licenses/by-nc-nd/4.0/

This article has been accepted for publication in IEEE Access. This is the author's version which has not been fully edited and
content may change prior to final publication. Citation information: DOI 10.1109/ACCESS.2025.3572554

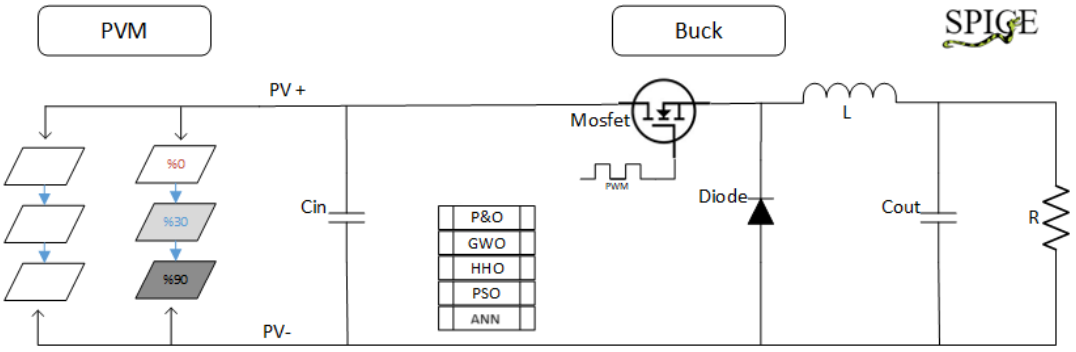


FIGURE 2. PySpice model for DC-DC buck converter

TABLE 2. Converter parameters

Components	State	Specification
Mosfet	Active	IRF150
Diode		1N5822
C_{in}	Passive	100 µF
C_{out}		10 µF
L		5 mH
R		10 Ω

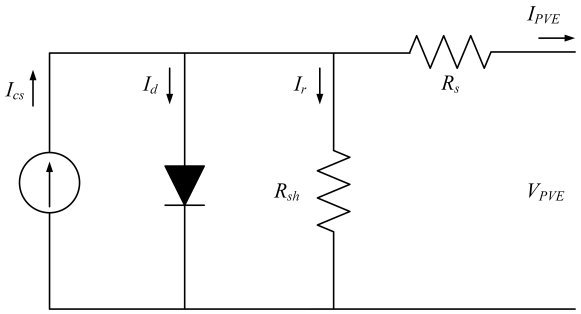


FIGURE 3. PV Array single diode equivalent circuit

using different optimization algorithms [35–37]. The PV equivalent circuit in Figure 3 is used to design theoretical PVM. The PV equivalent circuit can be mathematically modeled using Equations (1)-(5) after calculating the parameters I, I_{ph}, I_d, I_0, and I_r using polynomial equations [38].

$$I = I_{\text{ph}} - I_{\text{d}} - I_r \tag{1}$$

$$I_{\text{ph}} = I_{\text{sho}} \left(\frac{S}{1000} \right) + J_0 (T - T_{\text{ref}}) \tag{2}$$

$$I_d = I_0 \left[\exp \left(\frac{q(V + R_s I)}{nkT} \right) - 1 \right] \tag{3}$$

$$I_0 = I_{d0} \left(\frac{T}{T_{\text{ref}}} \right)^3 \exp \left(\frac{qE_g}{nk} \left(\frac{1}{T_{\text{ref}}} - \frac{1}{T} \right) \right) \tag{4}$$

$$I_r = \frac{V + R_s I}{R_{sh}} \tag{5}$$

S is the solar radiation in W/m^2, T_{ref} is the reference temperature at 298°K, T is the PV cell temperature, E_g is the energy band gap of the cell semiconductor, k is the Boltzmann constant, and n is the diode emission factor. R_s and R_{sh} are the series and shunt resistances, respectively. I, I_r, I_d, $I_{\text{L(ph)}}$, and I_0 are the array equivalent circuit current, the shunt resistance current, the diode current, the current generated by irradiance, and the reverse saturation diode current, respectively. I_{d0}, I_{sho}, and J_0 represent reverse diode current, short-circuit current, and temperature coefficient, respectively.

PVM, developed by De Soto et al. [39], is used in the Python development environment PVLIB [40] due to its success and ease of use. However, the PVM of PVLIB-De Soto is valid if the series-connected arrays operate under equal radiation. The PSC of one of the series-connected arrays significantly reduces the array current. Bypass diodes remove the array under PSC from the system until shading passes to prevent the series current from falling [41]. Therefore, the total power of the PV array decreases according to the shading rate. The characteristic curve of the arrays is distorted by the formation of local MPP (LMPP) due to PSC. There is a need for a second PVM that can reflect PSC. Therefore, a new PSC model was created by combining PVLIB-De Soto with the 0.8 V_{oc} PVM [42–44]. During the calculation of the main current passing through the series-connected modules in the 0.8 V_{oc} PVM, the voltages of the module V_{sub1} and V_{sub2} were calculated using Equations (6) and (7), considering the change in the radiation level. In the new PSC model created by modifying the PVLIB-De Soto PVM: First, three modules connected in series were calculated separately with the PVLIB-De Soto PVM. Then, the P-V and I-V characteristic curves for PSC were created by combining the currents through the first module at voltage V_{sub1}, the second module at V_{sub2}, and the third module at a higher voltage than V_{sub2}. G_1, G_2, and G_3 are the irradiance levels of the PV modules. N_1 and N_2 are the numbers of PV arrays receiving the corresponding irradiation. V_{oc} is the open-circuit voltage. A is a coefficient usually taken as 0.6347.

$$V_{\text{sub1}} = N_1 \left[V_{\text{oc}} + \frac{1}{A} \ln \left(1 - \frac{G_2}{G_1} \right) \right] \tag{6}$$

This work is licensed under a Creative Commons Attribution-NonCommercial-NoDerivatives 4.0 License.
For more information, see https://creativecommons.org/licenses/by-nc-nd/4.0/

This article has been accepted for publication in IEEE Access. This is the author's version which has not been fully edited and
content may change prior to final publication. Citation information: DOI 10.1109/ACCESS.2025.3572554

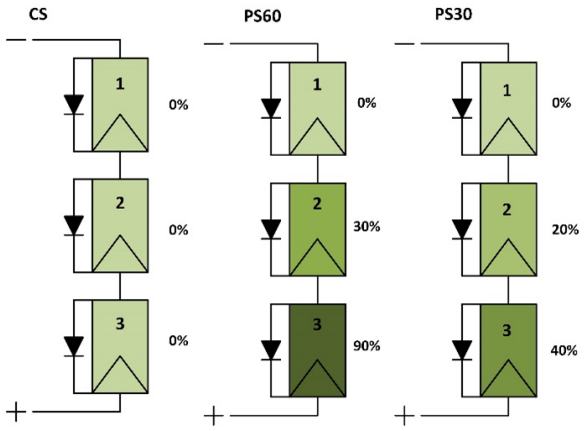


FIGURE 4. Uniform and non-uniform irradiance patterns

$$V_{\text{sub2}} = V_{\text{sub1}} + N_2 \left[V_{\text{oc}} + \frac{1}{A} \ln \left(1 - \frac{G_3}{G_2} \right) \right] \tag{7}$$

- **Introducing Shading Patterns**

The solar irradiation received under CSC, PSC60, and PSC30 are given in Figure 4. It is assumed that all three modules receive uniform irradiation under CSC. On the other hand, the shading percentages of the three modules for PSC60 are 0%, 30%, and 90% of the reference irradiance, and 0%, 20%, and 40% of the reference irradiance for PSC30. Uniform and non-uniform irradiance patterns are given in Table 3.

TABLE 3. The irradiance patterns with degrees of shading on the PV modules in PWM

PV	Shading [%]		
	CSC	PSC60	PSC30
Module 1	0	0	0
Module 2	0	30	20
Module 3	0	90	40

- **Generating PV Characteristics**

The V-P and V-I curves used in the simulation were generated under CSC and PSC, where 0%, 30%, and 90% shading was applied to a series of three panels under different irradiance levels. These curves were then compared for performance evaluation. Figure 5 shows the chart created using the data from this comparison. It is observed in Figure 5 that the V-I graph of the PSC model is formed in the form of steps according to the shading rates falling on the panels. Maximum power points formed within three digits in the knee regions on the I curve, but two of these three points formed LMPP, and the point in the second digit with the highest value formed the GMPP. If MPPT control algorithms are deceived by the LMPPs formed in the PSC model, losses may occur in the energy harvested in high-power solar power plants. That's why new optimization algorithms have been developed that can find GMPP and respond quickly to changes in the weather. Moreover, depending on the climatic conditions of the region in which the solar panel is installed, the levels of solar irradiance, ambient temperature, and shading on the panel surface are expected to vary throughout the day. Therefore, in our study, different solar panel models are operated with various radiation intensities, and the characteristic curves created for each situation are shown in Figure 5. When these curves are examined, the maximum power level formed at different radiation levels changes directly with the radiation level. Still, the change in the V_{MPP} value, that is, the occupancy rate in which GMPP is located, has remained at almost non-existent levels.

The characteristic curves obtained by operating the different solar panel models used in this study with various temperatures are given in Figure 6. If we compare Figure 5 and Figure 6, it is seen that the change in maximum power remains at low levels and the changes in V_{MPP} are many. Also, it is observed that the change in radiation generally shifts the curves in a vertical direction, while the curves change horizontally with the temperature change.

To better understand the differences between the two PVMs developed, the characteristic curves obtained under standard test conditions (1000 W/m^2, and 25°C) are given again in Figure 5. The decrease in the maximum power in Figure 6 that can be taken from the panel if the panel operates in the case of partial shading is visible. When Figure 6 is examined, although we encounter the highest current level in the first digit in the case of partial shading, only the LMPP is formed here because the voltage is low. In the third step of the voltage-current curve, although the voltage level increased, there were decreases in the current level this time, and at this point, the LMPP was formed. It is observed that GMPP is formed in the knee region of the second step, where the power value is the highest.

Table 4 gives the characteristic results of PVMs: 1000 W/m^2 solar irradiance and 25°C temperature for all modules in CSC, and 1000-700-100 and 25°C for the corresponding modules in PSC.

- **Artificial Neural Network**

The interest in ANN is increasing daily. It can be easily applied in various areas without having detailed information about the system's operation. Inspired by the structure of neural networks in the human brain, ANN models consist of many simple processing units connected. Each neuron generally consists of the number of input information determined by the user, the weight values to be updated later during training, the deviation coefficient that expresses the artificial neural limit value, and the activation function [25]. Equation (8) shows that a neuron uses these values to reach the result from the input values.

$$y_i = f \left(\sum_{j=1}^{n} w_{ij} \cdot x_j + b_i \right) \tag{8}$$

Where y_i is the activation function f, w is the weights, x is the input values, and b is the deviation coefficient. The ANN model training dataset is analyzed to establish a connection

This work is licensed under a Creative Commons Attribution-NonCommercial-NoDerivatives 4.0 License.
For more information, see https://creativecommons.org/licenses/by-nc-nd/4.0/

This article has been accepted for publication in IEEE Access. This is the author's version which has not been fully edited and content may change prior to final publication. Citation information: DOI 10.1109/ACCESS.2025.3572554

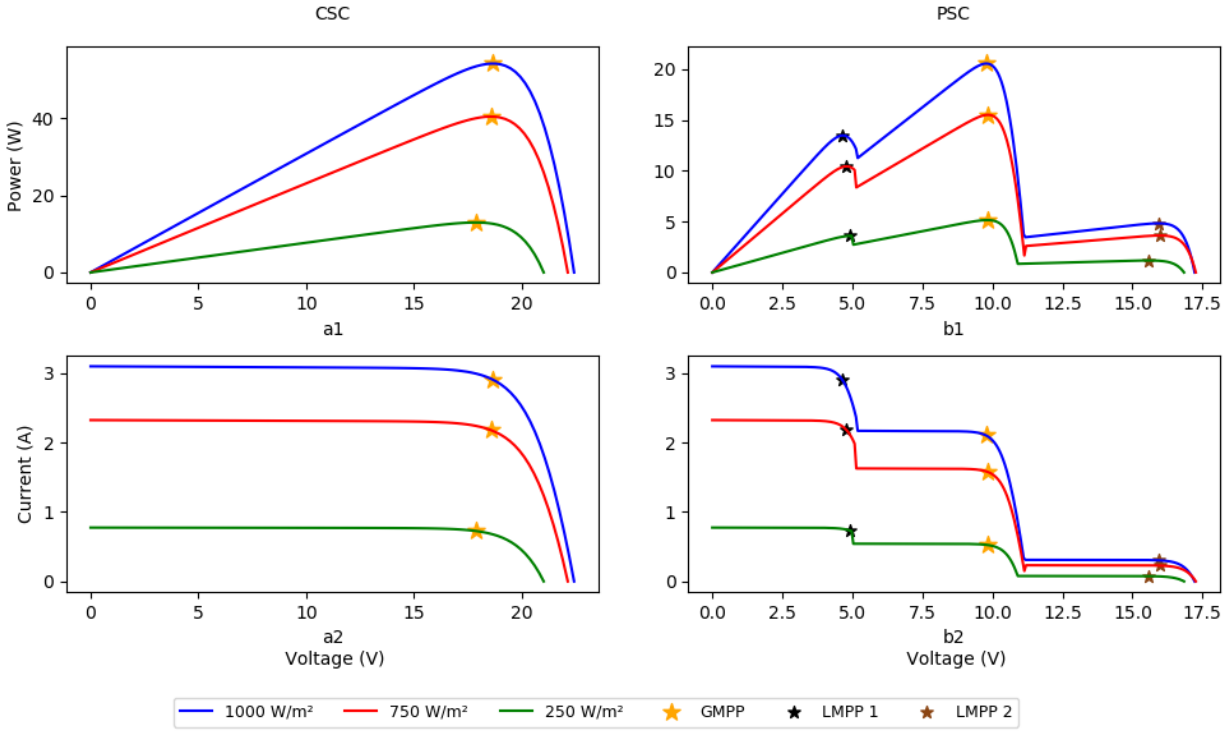


FIGURE 5. The characteristics of PVMs under different radiation

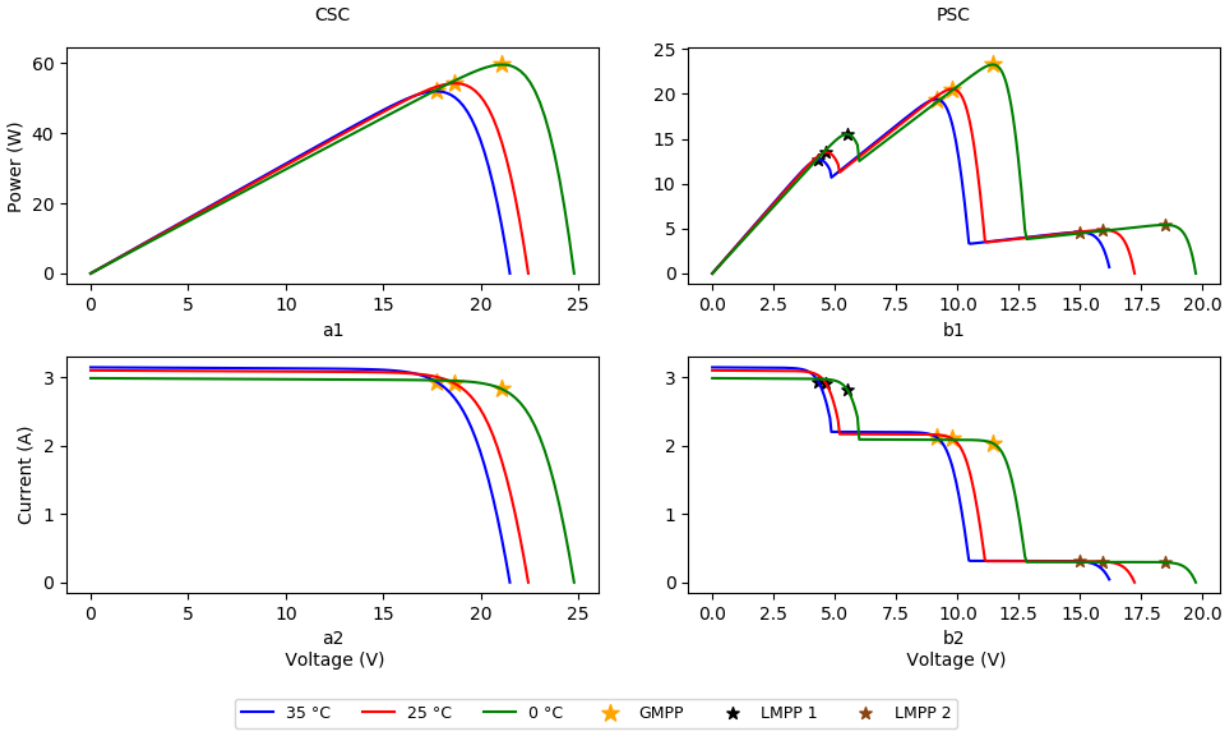


FIGURE 6. The characteristics of PVMs under different temperatures

This work is licensed under a Creative Commons Attribution-NonCommercial-NoDerivatives 4.0 License.
For more information, see https://creativecommons.org/licenses/by-nc-nd/4.0/

This article has been accepted for publication in IEEE Access. This is the author's version which has not been fully edited and content may change prior to final publication. Citation information: DOI 10.1109/ACCESS.2025.3572554

TABLE 4. The characteristic results of PWMs

PWM	P_{GMPP} [W]	V_{GMPP} [V]	P_{LMPP_1} [W]	V_{LMPP_1} [V]	P_{LMPP_2} [W]	V_{LMPP_2} [V]
CSC	54.26	18.68	-	-	-	-
PSC	20.54	9.77	13.47	4.64	4.83	15.93

between the input and the output values by the combination of a vast number of neurons, and the weight values are updated accordingly. Therefore, ANN can solve nonlinear problems, keep up with fast-changing conditions, and prevent the mistakes of conventional techniques [27]. The multi-layer perceptron (MLP) technique is one of the most widely used types of ANNs today. MLP has a forward-feed network structure [45]. The MLP backpropagation learning algorithm, trained on the training set, captures the nonlinear correlation between the input variables and the output and updates the weights [46]. Suppose the training dataset recurrently changes according to the complexity of the problem to be solved, and the MLP hyperparameters are appropriately tuned. In that case, the neural network can successfully find the result even if the input values are not given in the training set. Since testing the neural network using the training data will reflect the model's accuracy, the dataset has been divided into two parts: training and testing. The percentage of these parts also affect the model's success.

In this study, the ANN model to be used as the MPPT control algorithm was created by using MLP. The AI models and tools used are taken from the Scikit Learn library [47]. Compared to conventional MPPT methods such as P&O or IC, the ANN-based algorithm is more effective at managing the nonlinear behavior of PV systems, particularly under high-temperature conditions. This advantage stems from the neural network's ability to learn the specific current-voltage (I-V) characteristics of the PV module across a wide range of temperatures. Consequently, the optimal operating point is predicted more accurately than with existing methods, which rely on basic perturbation strategies.

The optimally configured ANN follows an architecture consisting of one input layer, three hidden layers, and one output layer. The training process aims to minimize the error between the predicted and actual duty cycle by adjusting the network's weights and biases. Accordingly, the flowchart of the proposed methodological framework is presented in Figure 8. The training and testing data set was obtained from the results in different situations created in the simulation environment. This study systematically evaluated the performance of P&O, GWO, HHO, and PSO under varying irradiance and temperature conditions.

As shown in Figure 8, weather data were generated by cross-combining seventy-five irradiance levels ranging from 100 to 1000 W/m² and fourteen temperature levels from $-10\,^{\circ}\mathrm{C}$ and $50\,^{\circ}\mathrm{C}$. These combinations were processed using four optimization algorithms and two solar panel models, resulting in a dataset containing over 8000 samples for the

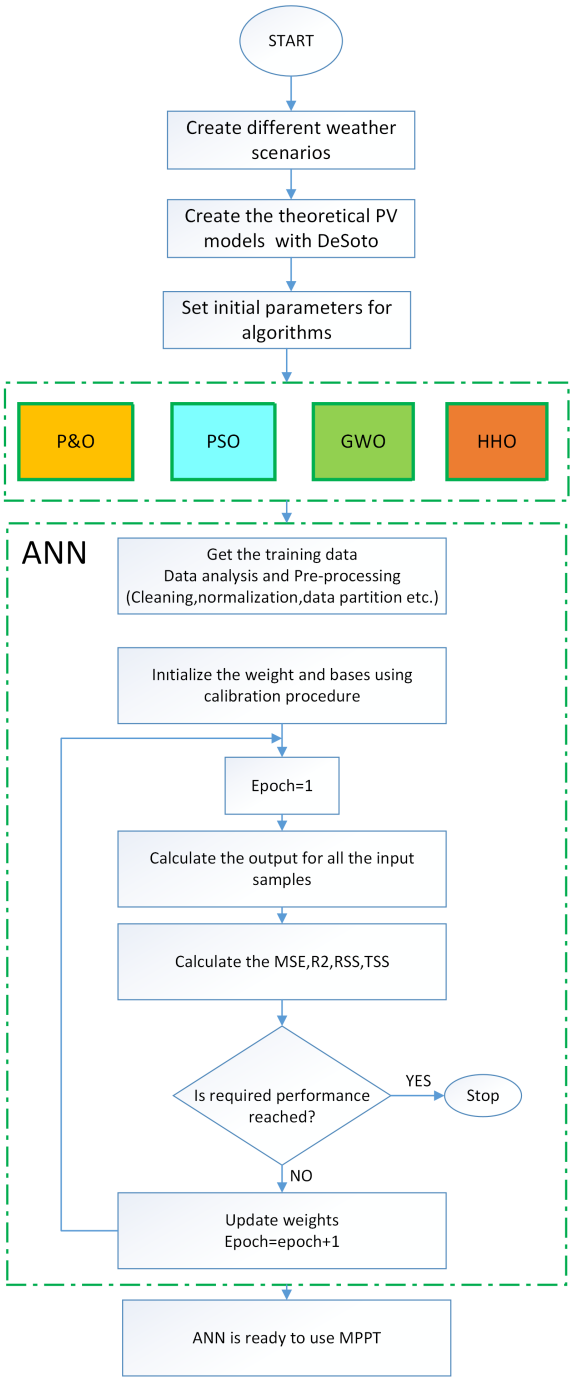


FIGURE 8. Flowchart of the proposed method

This work is licensed under a Creative Commons Attribution-NonCommercial-NoDerivatives 4.0 License.
For more information, see https://creativecommons.org/licenses/by-nc-nd/4.0/

This article has been accepted for publication in IEEE Access. This is the author's version which has not been fully edited and
content may change prior to final publication. Citation information: DOI 10.1109/ACCESS.2025.3572554

ANN model. The values obtained in the simulation results with the P&O for partial shading were excluded from the data set because they were below the expected value. In detail, the dataset was structured with three input features: irradiance, temperature, and MPPT algorithm type, and a single output variable: the optimal duty cycle corresponding to the MPP. To enhance data quality, anomalous values that could negatively affect training are identified and removed through outlier detection techniques. In cases where missing values (e.g., absent irradiance or temperature readings) are encountered, interpolation techniques are applied to fill these gaps without introducing bias. Prior to training, the input features were scaled using 'StandardScaler' to normalize the data distribution. The data are standardized to improve model performance and stabilize the learning process using a standard scaler function, ensuring a mean of 0 and a standard deviation of 1. In this regard, the dataset used to train and test the ANN model for MPPT is comprehensive and encompasses various environmental conditions, PV system configurations, and geographical locations. The data were selected to represent both optimal and suboptimal operating conditions for PV systems. After the dataset is created, random data is separated from this dataset using train test split, which is one of the Scikit-learn functions. 80% of the data is used for training, and 20% is used for testing.

On the other hand, a metaheuristic algorithm was integrated into the systematic framework to enhance the training process of the ANN. The specific metaheuristic method employed is PSO, which was applied in conjunction with grid search (GS) to optimize the weights of the ANN. PSO was selected due to its capability to efficiently explore a vast solution space and its ability to avoid local minima that may hinder convergence to the optimal solution. On the other hand, the PSO was employed to initialize the weights and biases of the ANN to enhance convergence speed and avoid local minima during training. Conversely, the P&O was used to establish baseline operating conditions and to generate reference MPP patterns, which helped in improving the generalization of the ANN. Overall, the training process involved two phases: (1) weight and bias initialization using PSO to accelerate convergence and escape local minima, and (2) fine-tuning the model using GS-cross validation (CV) to optimize hyperparameters. Here, the purpose of hyperparameter optimization is to improve the model's ability to predict the MPP under varying environmental conditions accurately. In this context, the hyperparameters of the ANN model are fine-tuned to identify the optimal configuration that yields the best performance for the MPPT. In this process, multiple combinations of hyperparameters such as activation functions ('logistic', 'relu'), regularization strength (alpha: 0.01, 0.02, 0.05), and hidden layer architectures (e.g., (100, 50, 150), (300, 200, 250)) were systematically evaluated. These parameters enhance the model's learning capacity, while the activation function determines how well the model captures nonlinear relationships and must be appropriately selected to ensure accurate and efficient training. Thus, selecting a successful activation function that is appropriate to the model is essential. Today, the rectified linear unit (ReLU) function, considered one of the most successful activation functions, is commonly used by academicians and researchers. Although they proposed a new alternative to replace ReLU, these new methods were not preferred due to indecisiveness. The simplicity and success of ReLU have become a significant milestone in the training of deep learning models [47]. The activation function formula of the ReLU is described in Equation (9).

$$f(x) = \max(x, 0) \tag{9}$$

The learning rate, which controls the extent to which weights are updated during training, is crucial for achieving optimal convergence without overshooting the optimal solution. The batch size, which defines the number of training samples processed before the model's weights are updated, is incorporated into the systematic framework with values of 32, 64, and 128. The number of epochs, representing how many times the entire dataset is passed through the model, is considered with values of 100, 200, and 300 in order to determine the optimal number of training iterations before overfitting occurs. Another critical aspect is the choice of the optimization algorithm, which directly affects the convergence rate of the model. Since the performance of optimization algorithms can vary depending on the complexity of the problem, optimizers such as Adam, RMSProp, and Stochastic Gradient Descent (SGD) were considered in this study, with Adam ultimately being selected. Adam has features such as being easy to apply, swift and efficient in working, and having a low memory requirement. Therefore, it successfully solves problems with high data and parameters [48]. It is well-known for its computational efficiency and robustness in handling sparse gradients and noisy data. Adam combines the advantages of both RMSProp and momentum by maintaining separate moving averages of the gradients (first moment) and squared gradients (second moment) for each parameter. The update rule is adjusted using bias correction terms, particularly in the early training stages, to ensure more reliable convergence. Mathematically, the algorithm utilizes two exponential decay rates: β_1 (typically set to 0.9) for the momentum term and β_2 (often set to 0.999) for the second moment estimate. These hyperparameters allow the optimizer to adaptively adjust the step sizes for each parameter based on their historical gradients. A learning rate of 0.01 was selected based on empirical tuning, whereas the default values for the exponential decay rates ($\beta_1 = 0.9$, $\beta_2 = 0.999$) were preserved, given their consistently strong performance across various neural network applications in the literature. The search space for hyperparameter optimization is constructed using GS-CV, covering all possible combinations of defined parameter ranges. A 10-fold CV was applied to ensure generalizability and to avoid overfitting during the hyperparameter search. With the help of the GS-CV function, a large number of various hyperparameters introduced into the model are cross-validated among themselves

This work is licensed under a Creative Commons Attribution-NonCommercial-NoDerivatives 4.0 License.
For more information, see https://creativecommons.org/licenses/by-nc-nd/4.0/

This article has been accepted for publication in IEEE Access. This is the author's version which has not been fully edited and
content may change prior to final publication. Citation information: DOI 10.1109/ACCESS.2025.3572554

to find values that work most harmoniously and successfully with each other [48]. The block diagram in Figure 9 contains the MLP model created using the GS-CV. The radiation and temperature variables in the input layer of the developed model represent the duty cycle used for the switching element of the DC/DC converter in the result layer.

After developing the MLP model and evaluating its resource requirements, the training process was conducted using mini-batches of size 64 to balance convergence speed and stability. The model was trained on the training dataset, and its performance was evaluated using the Mean Squared Error (MSE) and R-squared (R^2) metrics from the Scikit-Learn library. MSE quantifies the average squared difference between the predicted and actual values, serving as a signal similarity criterion. In this study, the ANN-predicted duty cycles were compared with reference values in the test set, and the squared errors were averaged to calculate MSE, as shown in Equation 10. To find the optimal configuration, various hyperparameter combinations were tested. The best validation performance was obtained using the ReLU activation function, an α value of 0.01, and a network structure with three hidden layers containing 100, 50, and 150 neurons, respectively. Once the optimal hyperparameters were identified, the model was retrained on the entire training dataset and evaluated on the test set. During training, forward propagation computed the network output using current weights and biases, while backpropagation calculated gradients of the loss function with respect to each parameter. The Adam optimizer used these gradients to update the model parameters. To enhance generalization and prevent overfitting, ℓ_2 regularization was applied with an α of 0.01. An early stopping mechanism was also implemented to terminate training if no improvement was observed within a defined number of iterations. The training was allowed to run up to 1000 iterations, and 10% of the training data was allocated for internal validation. The final ANN model was compared with traditional and metaheuristic techniques, demonstrating superior performance in terms of tracking accuracy and robustness. The model captured the nonlinear relationship between environmental variables (irradiance and temperature) and the desired output (duty cycle), as indicated by high R^2 and low RMSE values on the test set. The R^2 value, or stability coefficient, reflects the model's ability to fit the data's variability, with a higher value demonstrating better generalization. The R^2 value was calculated using Equation (11).

The implementation was carried out using Python 3.11 on a Windows 11 system equipped with an Intel Core i7-12700H CPU, 32 GB RAM, and an NVIDIA RTX 3060 GPU. However, since Scikit-learn's MLPRegressor does not support GPU acceleration, the training was executed on the CPU. To support reproducibility and future research, all code and datasets are available upon request. Detailed performance evaluations for each algorithm are presented in Section ref sec: Simulation Results and Discussion.

The proposed methodological framework is highly useful in terms of reproducibility. In terms of training parameters, the final epoch value considered in the ANN model was selected according to the GS. The training process is stopped if the validation error does not improve after a predefined number of epochs. Regarding batch size, the optimal final value for the ANN model is determined within the search space based on available computational resources and training speed. The Adam optimizer was used for training the model due to its ability to adaptively adjust learning rates for each parameter, making it highly suitable for training deep learning models. The loss function used for training was MSE, which is commonly employed for such regression tasks. Another approach to prevent overfitting and ensure proper convergence of the model is early stopping. If the validation loss does not improve after a certain number of epochs, training is halted, with the patience parameter used to control this behavior. High-performance computing resources, specifically GPU capabilities, were utilized to train the model and perform hyperparameter optimization. The use of GPUs significantly reduces training time, especially for the ANN model, which has a relatively large number of parameters. In the simulation environment, various Python libraries that are widely accessible to many users were used for data preprocessing, neural network construction and training, and hyperparameter optimization.

An important aspect of the proposed model, alongside its training and reproducibility, is the efficient management of computational complexity and resource requirements. In this regard, the model does not introduce significant computational complexity in terms of the number of neurons, hidden layers, and the size of the training dataset. Specifically, for hyperparameter tuning, the number of hidden layers is considered up to three, the number of neurons is considered up to 300, and the training dataset size is considered up to 8000 samples. Ultimately, the time required for training the ANN model does not increase the resource demand, as it depends on several factors, including the number of hyperparameter combinations tested. On average, the training process took approximately 2.5 hours for a dataset with 8000 data points. On the other hand, compared to existing MPPT methods such as P&O and IC, the ANN-based method requires significantly more computational resources during the training phase but provides superior performance in terms of tracking accuracy and robustness in dynamic environments. Traditional methods like P&O rely on relatively simple algorithms that require only basic arithmetic operations and have a low computational load. These methods are fast and effective in real-time operations, but may experience slower response times or incorrect tracking issues under rapidly changing environmental conditions. Another consideration is the processing power and time required by the model. The ANN-based MPPT method requires more processing power due to the need for matrix operations during the forward pass and training process. However, once the model is trained, the inference time (making a prediction) is typically faster than traditional methods because the ANN can evaluate the optimal power

This work is licensed under a Creative Commons Attribution-NonCommercial-NoDerivatives 4.0 License.
For more information, see https://creativecommons.org/licenses/by-nc-nd/4.0/

This article has been accepted for publication in IEEE Access. This is the author's version which has not been fully edited and
content may change prior to final publication. Citation information: DOI 10.1109/ACCESS.2025.3572554

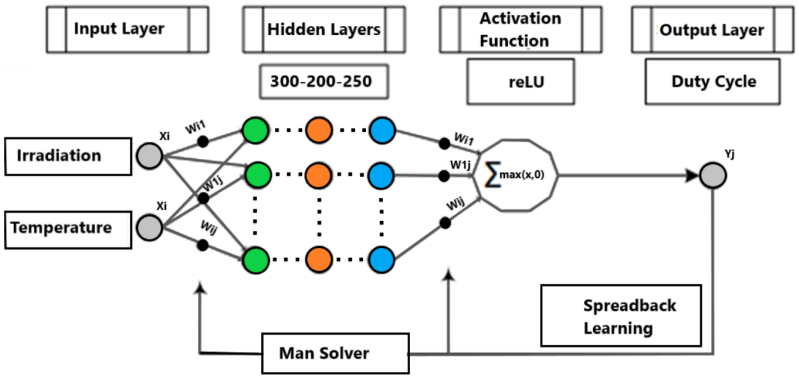


FIGURE 9. Architecture of the MLP Model

point more quickly through parallel computation. In contrast, methods like P&O and IC are typically executed in real-time with simpler hardware and lower processing power. These traditional algorithms require minimal computational resources and shorter execution times (typically on the order of milliseconds per iteration), which makes them widely used in embedded systems with limited resources. Overall, the main trade-off when using the ANN-based method is the higher computational cost during the training phase, which may limit its use in systems with constrained resources or when real-time retraining is required. However, once the ANN model is trained, its real-time operation is efficient, and it can outperform traditional methods, particularly in terms of accuracy and robustness under changing environmental conditions.

$$\text{MSE}(x, y) = \frac{1}{N}\sum_{i=1}^{N}(x_i - y_i)^2 \tag{10}$$

$$R^2 = 1 - \frac{\text{RSS}}{\text{TSS}} \tag{11}$$

$$\text{RSS} = \sum_{i=1}^{N}(x_i - y_i)^2 \tag{12}$$

$$\text{TSS} = \sum_{i=1}^{N}(y_i - \bar{y})^2 \tag{13}$$

The Residual Sum of Squares (RSS) represents the sum of the squared differences between the observed values in the test set and the corresponding values predicted by the model, and is computed according to Equation (12). The Total Sum of Squares (TSS) refers to the sum of squared deviations for the variable's total variation, as defined in Equation (12). It is calculated by summing the squares of the differences between the actual values (y) in the dataset and the mean of all observations. The ratio of RSS to TSS quantifies the proportion of variability that the model fails to account for. By subtracting this ratio, which ranges from 0 to 1, and applying the transformation defined in Equation (13), we derive the model's effectiveness in capturing and explaining the observed variability.

III. PERFORMANCE METRICS

In evaluating the performance of tracking and control algorithms, several performance indices are commonly used to quantify the accuracy and efficiency of the system. These indices include the Integral of Squared Error (ISE), Integral of Time-Squared Error (ITSE), Integral of Absolute Error (IAE), and Integral of Time-Absolute Error (ITAE). Each of these indices plays a significant role in assessing different aspects of the system's behavior. The Integral of Squared Error (ISE) is a widely used performance metric that emphasizes large deviations by squaring the error at each point in time. The ISE is calculated by integrating the squared error over time as follows:

$$\text{ISE} = \int_0^T e(t)^2\, dt \tag{14}$$

where $e(t)$ is the error signal at time t, and T is the total observation time. The ISE penalizes larger errors more heavily and is useful when aiming for minimal overall error. The ITSE is similar to ISE but includes a time-weighting factor, which gives more importance to errors that occur later in the process. The formula for ITSE is given by:

$$\text{ITSE} = \int_0^T t \cdot e(t)^2\, dt \tag{15}$$

In this expression, t is the time factor, and the time-weighted error ensures that errors occurring at later stages in the process are penalized more significantly. The IAE calculates the total accumulated absolute error over time. Unlike ISE, which squares the error, IAE gives equal importance to all errors, regardless of their magnitude. The formula for IAE is:

$$\text{IAE} = \int_0^T |e(t)|\, dt \tag{16}$$

This index is useful when it is desirable to maintain a more uniform treatment of errors, avoiding excessive penalty for large deviations, and ensuring a balanced overall error measure.

The ITAE is similar to the IAE but with an additional time-weighting factor, which means that errors persisting over

This work is licensed under a Creative Commons Attribution-NonCommercial-NoDerivatives 4.0 License.
For more information, see https://creativecommons.org/licenses/by-nc-nd/4.0/

This article has been accepted for publication in IEEE Access. This is the author's version which has not been fully edited and
content may change prior to final publication. Citation information: DOI 10.1109/ACCESS.2025.3572554

time are penalized more heavily. The ITAE is calculated as:

$$\text{ITAE} = \int_0^T t \cdot |e(t)|\, dt \tag{17}$$

Here, t is the time variable, and $|e(t)|$ is the absolute error. The ITAE places a higher penalty on errors that persist over longer durations, making it useful for ensuring quick convergence and minimizing steady-state errors. These performance metrics are designed to evaluate different characteristics of the system's error behavior. While ISE and ITSE focus on the squared error, they vary in the weight given to errors occurring later. IAE and ITAE, on the other hand, use the absolute error but differ in how they treat the impact of time. The choice of performance metric depends on the specific system requirements, such as the need for quick convergence, minimal steady-state error, or sensitivity to large deviations.

IV. SIMULATION RESULTS AND DISCUSSION

This section provides a detailed analysis of the simulation results. The simulation was developed using the PySpice and Pvlib libraries in a Python program, and the performance of the optimization algorithms was evaluated extensively. P&O was run over 20 iterations using 50 steps, while GWO, HHO, and PSO were run through 20 iterations using 5 search agents. The ANN optimization algorithm, developed with these four algorithms and the AI model trained with the results obtained from these algorithms, was tested in the weather conditions given in Table 3. A comparison was made with conventional P&O and metaheuristic-based techniques to evaluate the performance of the proposed ANN-based MPPT algorithm under uniform and non-uniform shading conditions. In addition, the performance of the proposed ANN-based optimization algorithm was assessed by comparing it with the results obtained in our previous study [49], which conducted a comprehensive comparative analysis of MPPT strategies and their daily performance under dynamic environmental conditions.

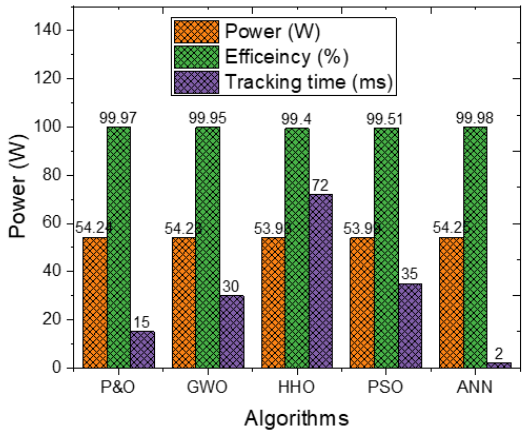


FIGURE 10. Performance evaluation of ANN and others under uniform condition

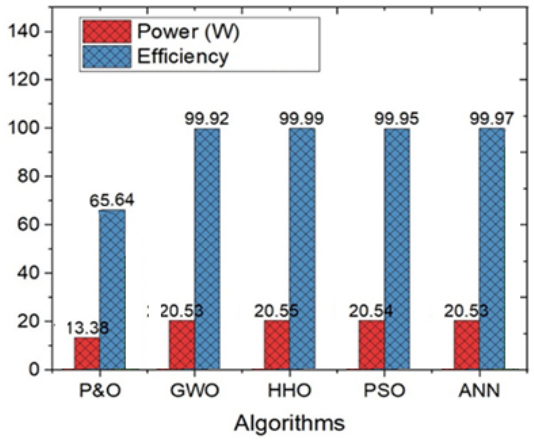


FIGURE 11. Performance evaluation of ANN and others under non-uniform irradiation, partial shading

Figure 11 presents the success graph obtained from tests conducted using the PSC model. However, the performance evaluation of ANN and other algorithms under uniform conditions, as shown in Figure 10, is not included in Figure 11 due to significant discrepancies in algorithm tracking times. Instead, these results are provided in Table 6. Under uniform shading (Figure 10), the ANN algorithm achieved the highest power output (54.25 W) and efficiency (99.98%), alongside the fastest tracking time (0.002 s). Additionally, ANN exhibited superior precision with error metrics close to zero, reflecting excellent convergence. While the P&O and GWO also demonstrated high efficiency, they showed slower convergence rates compared to ANN. Under non-uniform shading conditions (Figure 11), the ANN algorithm continued to maintain high performance, delivering 20.53 W of power and 99.97% efficiency, with a quick convergence time of 0.092 s. Although the P&O was faster in tracking (0.047 s), its power output was significantly lower (13.38 W) with reduced efficiency (65.64%), primarily due to its inability to handle the multiple peaks caused by partial shading. The HHO provided slightly higher power (20.55 W) but suffered from an impractically long tracking time (706 s). PSO achieved competitive power (20.54 W) and efficiency (99.95%), though it required a longer convergence time (150 s). Tables 5 and 6 provide a comprehensive overview of these key performance metrics. These results underscore the ANN model's exceptional adaptability and precision, particularly under complex shading conditions. The hybrid training approach, combining analytical and metaheuristic optimization techniques, allows the ANN to deliver fast convergence with minimal steady-state error, surpassing both conventional and heuristic-based algorithms in dynamic shading environments. A comparative analysis was conducted to assess the robustness and effectiveness of the proposed ANN-based MPPT algorithm under both uniform and partial shading conditions. The performance indices for the ANN approach were compared with those of conventional (P&O) and metaheuristic-based techniques, as summarized in Tables 5 and 6. Under uni-

This work is licensed under a Creative Commons Attribution-NonCommercial-NoDerivatives 4.0 License.
For more information, see https://creativecommons.org/licenses/by-nc-nd/4.0/

This article has been accepted for publication in IEEE Access. This is the author's version which has not been fully edited and
content may change prior to final publication. Citation information: DOI 10.1109/ACCESS.2025.3572554

TABLE 5. Performance Indices Under Uniform Shading

Algorithm	P_mpp (W)	Efficiency (%)	Tracking Time (s)	ISE	ITSE	IAE	ITAE
P&O	54.24	99.97	0.015	0.0001	0.000002	0.01	0.00015
GWO	54.23	99.95	0.030	0.0004	0.000012	0.02	0.00060
HHO	53.93	99.40	0.072	0.1024	0.007373	0.32	0.02304
PSO	53.99	99.51	0.035	0.0676	0.002366	0.26	0.00910
ANN	54.25	99.98	0.002	0.0000	0.000000	0.00	0.00000

TABLE 6. Performance Indices Under Non-Uniform Shading

Algorithm	Power (W)	Efficiency (%)	Tracking Time (s)	ISE	ITSE	IAE	ITAE
P&O	13.38	65.64	0.047	51.2656	2.409483	7.16	0.33652
GWO	20.53	99.92	67.33	0.0001	0.006733	0.01	0.6733
HHO	20.55	99.99	706.0	0.0001	0.0706	0.01	7.06
PSO	20.54	99.95	150.0	0.0000	0.0000	0.0000	0.0000
ANN	20.53	99.97	0.092	0.0001	0.000009	0.01	0.00092

form shading (Table 5), the ANN demonstrated superior performance, achieving the highest maximum power point (54.25 W), the fastest tracking time (0.002 s), and the highest efficiency (99.98%). Additionally, the performance indices were zero or near-zero, indicating precise tracking and stable convergence. Although both GWO and P&O showed high efficiency and low error, their convergence speeds were slower than that of the ANN. Conversely, HHO and PSO displayed higher error metrics, likely due to overshooting or oscillatory convergence behavior. In PSCs (Table 6), the ANN maintained strong performance. While HHO achieved slightly higher power (20.55 W), its tracking time (706 s) was significantly longer. ANN, however, converged in only 0.092 s, maintaining high power (20.53 W) and efficiency (99.97%), with minimal error metrics, indicating effective global search and accurate tracking in complex conditions. The conventional P&O, although faster in tracking (0.047 s), failed to identify the GMPP under PSC, resulting in lower power output (13.38 W) and efficiency (65.64%). Its local search nature hindered its ability to manage the multiple peaks induced by partial shading. Additionally, high error metrics such as ISE (51.27), ITSE (2.41), IAE (7.16), and ITAE (0.34) indicated poor tracking accuracy and unstable convergence, further highlighting the limitations of the P&O in dynamic shading scenarios. In summary, the results highlight the ANN-based MPPT approach's superior adaptability and precision across diverse operating conditions. Its hybrid training mechanism, combining analytical and metaheuristic optimization techniques, enables robust global search, rapid convergence, and minimal steady-state error, distinguishing it from both conventional and heuristic-based methods, particularly in dynamic and challenging shading environments.

Table 7 presents a comprehensive comparison of the dynamic tracking performance of various MPPT algorithms, including classical methods, metaheuristic approaches, and an ANN. The evaluation is carried out under three different PVM configurations (CS, PS60, and PS30) and across three irradiance scenarios denoted as K, L, and M. The reference power represents the theoretical maximum power output under ideal tracking, whereas the maximum power columns indicate the actual power extracted by each algorithm. Across all configurations and scenarios, the ANN-based method consistently achieves power values nearly identical to the reference, indicating near-optimal performance. In contrast, traditional P&O demonstrates significant power loss, especially under PS60 and PS30, due to its slower response and susceptibility to local optima. The efficiency values reflect the ratio of the extracted power to the reference power. ANN and metaheuristic algorithms achieve very high efficiencies (close to or exactly 100%) under CS and even under more dynamically challenging scenarios like PS60 and PS30. Notably, ANN achieves an average efficiency of 99.87% under CS conditions and maintains above 99.5% efficiency under PS60 and PS30, outperforming all other methods. Traditional P&O underperforms with an average efficiency as low as 50.91% under PS30, indicating its limited suitability in highly dynamic or partial shading conditions. Tracking time is a critical parameter in assessing the responsiveness of MPPT algorithms. While metaheuristic algorithms exhibit high efficiency, their convergence times are significantly longer. For example, HHO requires a total of 10,485 s under PS30, and PSO takes 5,150 s under the same condition. In contrast, the ANN-based method exhibits substantially faster convergence, requiring only 25 s under CS and 128 s under PS30. This demonstrates that the ANN model not only maintains high accuracy but also offers real-time responsiveness, a critical feature for practical implementation in fast-changing environments. In summary, the ANN-based MPPT approach shows superior performance across all evaluated metrics. It achieves near-perfect efficiency with significantly reduced tracking times compared to traditional and metaheuristic methods. These results underline the potential of machine learning-based strategies in addressing the challenges of dynamic MPPT, particularly in real-time and partially shaded conditions.

Table 8 provides a comparative analysis of the daily performance of various MPPT algorithms based on real meteorological data, including solar irradiance and ambient

This work is licensed under a Creative Commons Attribution-NonCommercial-NoDerivatives 4.0 License.
For more information, see https://creativecommons.org/licenses/by-nc-nd/4.0/

This article has been accepted for publication in IEEE Access. This is the author's version which has not been fully edited and
content may change prior to final publication. Citation information: DOI 10.1109/ACCESS.2025.3572554

TABLE 7. Comparative Evaluation of MPPT Strategies under Dynamic Conditions

Method	PVM	Ref. Power (W)			Max. Power (W)			Efficiency (%)			Avg. Eff. (%)	Tracking time (s)			Total tracking time (s)
		K	L	M	K	L	M	K	L	M		K	L	M	
P&O	CS	3.64	9.43	5.56	3.54	9.33	5.48	97.33	98.93	98.56	98.28	20	49	79	148
	PS60	1.82	4.68	2.78	1.21	3.06	1.79	66.42	65.39	64.28	65.36	14	37	60	111
	PS30	2.56	6.52	3.89	1.28	3.29	2.03	49.99	50.49	52.25	50.91	15	42	64	121
HHO	CS	3.64	9.43	5.56	3.64	9.37	5.54	100.0	99.38	99.70	99.69	3227	3582	2666	9475
	PS60	1.82	4.68	2.78	1.82	4.65	2.76	100.0	99.30	99.51	99.60	2908	2483	2711	8102
	PS30	2.56	6.52	3.89	2.56	6.44	3.49	100.0	98.67	89.66	96.11	3675	3519	3291	10485
PSO	CS	3.64	9.43	5.56	3.64	9.39	5.44	100.0	99.63	97.89	99.17	1459	1552	1560	4571
	PS60	1.82	4.68	2.78	1.81	4.66	2.78	99.53	99.66	100.0	99.73	1088	1166	1362	3616
	PS30	2.56	6.52	3.89	2.55	6.46	3.89	99.87	98.95	100.0	99.61	1595	1770	1785	5150
GWO	CS	3.64	9.43	5.56	3.55	9.34	5.37	97.52	99.11	96.61	97.75	1320	1368	1396	4084
	PS60	1.82	4.68	2.78	1.82	4.36	2.74	100.0	93.20	98.77	97.32	1077	1226	1148	3451
	PS30	2.56	6.52	3.89	2.56	6.34	3.89	100.0	97.10	100.0	99.03	1670	1816	1738	5224
ANN	CS	3.64	9.43	5.56	3.64	9.41	5.55	100.0	99.79	99.82	99.87	6	7	12	25
	PS60	1.82	4.68	2.78	1.81	4.66	2.77	99.45	99.57	99.64	99.55	16	40	61	117
	PS30	2.56	6.52	3.89	2.56	6.51	3.85	100.0	99.85	99.00	99.62	18	44	66	128

temperature. The simulations were conducted using minutely averaged values recorded at the Department of Electrical Engineering, Yıldız Technical University, thereby ensuring realistic operating conditions for assessing algorithm robustness under dynamically changing environmental conditions. The table includes performance metrics under three irradiance scenarios: CS, 60% PS60, and 30% PS30. Metrics reported are harvested daily energy, efficiency, average efficiency across scenarios, and total runtime. Across all conditions, metaheuristic algorithms, such as PSO and GWO, deliver high energy harvesting efficiency, exceeding 97% on average. However, these algorithms tend to require significant computational time, particularly under dynamic shading conditions. For example, HHO exhibits strong accuracy but a prohibitively long runtime, reaching over 40,000 s under PS30. The conventional P&O performs acceptably under uniform irradiance, showing only a small efficiency gap (approximately 2%) relative to the metaheuristics. However, its performance significantly deteriorates under partial shading, with harvested energy falling below 66% and 62% of its CS value under PS60 and PS30, respectively. This degradation is attributed to the gradient-based nature of P&O, which makes it prone to getting trapped in LMPP during non-uniform irradiance. In contrast, the proposed ANN-based approach demonstrates strong generalization and adaptive capabilities. It maintains high energy harvesting rates and achieves average efficiencies exceeding 98% across all shading scenarios, while also delivering substantially lower computational costs. For instance, its total runtime remains below 65 s, significantly outperforming all other methods in time efficiency. The ANN's hybrid structure, combining analytical and data-driven techniques, enables it to respond quickly and accurately to real-time changes, making it highly suitable for practical deployment in variable field conditions. These findings underscore the practical advantage of the ANN-based estimator, particularly in environments with frequent irradiance fluctuations. While metaheuristic methods are effective in accuracy, the ANN provides a superior balance between performance and runtime, offering a compelling solution for real-time MPPT in photovoltaic systems.

The power, efficiency, and runtime results are presented in Figures 10 and 11, which illustrate the performance of the optimization algorithms under various weather conditions using PVMs in the simulation environment. The ANN-based algorithm exhibits high MPPT efficiency, achieving 99.98% under CSC and 99.97% under PSC, as confirmed by extensive simulations conducted on PVMs using efficiency evaluation metrics. Although the harvested energy and efficiency values obtained from the performance comparison between ANN and other heuristic algorithms are quite similar, ANN demonstrates a significantly shorter tracking duration, indicating faster dynamic response. On the other hand, under PSC scenarios, the ANN achieves notably higher harvested energy and efficiency compared to the analytical P&O. However, due to P&O's tendency to become trapped in local minimum, the tracking duration of ANN is slightly longer in this case.

V. CONCLUSION

This paper introduces an ANN-based MPPT algorithm designed to address the challenges posed by partial shading conditions in photovoltaic systems. The proposed algorithm demonstrates significant advantages over existing methods by incorporating advanced machine learning techniques and an adaptive approach capable of handling dynamic shading scenarios. These enhancements result in superior performance in terms of tracking accuracy, convergence speed, and stability. The analysis of the proposed ANN-based MPPT algorithm under both uniform and PSC reveals its exceptional adaptability and precision. Specifically, under uniform shading conditions, the ANN achieved the highest power output (54.25 W) and efficiency (99.98%) with the fastest tracking time (0.002 s). It also exhibited near-zero error metrics, indicating excellent convergence. In comparison, conventional

This work is licensed under a Creative Commons Attribution-NonCommercial-NoDerivatives 4.0 License.
For more information, see https://creativecommons.org/licenses/by-nc-nd/4.0/

This article has been accepted for publication in IEEE Access. This is the author's version which has not been fully edited and
content may change prior to final publication. Citation information: DOI 10.1109/ACCESS.2025.3572554

TABLE 8. Comparison of the Daily Performance of MPPT Algorithms: A Focus on ANN-Based Optimization

	CS	PS60	PS30	Harvested Energy [Wh/d]	Efficiency [%]	Avg. Efficiency [%]	Runtime (s)
P&O	×			63.71	97.54	71.94	418.91
		×		21.84	65.59		237.47
			×	24.39	52.68		242.66
HHO	×			63.82	97.66	97.11	14872.00
		×		32.29	96.98		20652.71
			×	44.76	96.69		40985.00
PSO	×			64.63	98.94	98.10	10337.99
		×		32.61	97.94		19040.57
			×	45.10	97.42		17545.02
GWO	×			64.60	98.81	97.92	1303.43
		×		32.48	97.54		2075.00
			×	45.10	97.41		8006.28
ANN	×			64.72	99.08	98.37	58.63
		×		32.69	98.26		64.13
			×	45.20	97.62		64.81

Note: Reference energy values are 65.32 (CS), 33.27 (PS60), 46.3 (PS30) Wh.

methods like P&O and GWO showed slower convergence rates, while algorithms like HHO and PSO suffered from higher error values due to overshooting and oscillatory behaviors. Under non-uniform shading conditions, the ANN maintained robust performance, delivering 20.53 W of power with 99.97% efficiency and a quick convergence time of 0.092 s. Although the P&O was faster (0.047 s), it struggled to handle multiple local maxima caused by partial shading, resulting in significantly lower power output (13.38 W) and reduced efficiency (65.64%). The HHO, while achieving slightly higher power (20.55 W), exhibited impractically long tracking times (706 s). Similarly, PSO achieved competitive results with 20.54 W of power and 99.95% efficiency, but required a considerably longer convergence time (150 s). These findings demonstrate the superior tracking precision and dynamic adaptability of the ANN in complex and non-uniform shading environments. Looking ahead, several avenues for future research can be explored to further enhance the performance of the ANN-based MPPT algorithm. These include hardware implementation for real-world validation, extensive field testing under diverse environmental conditions, and further optimization to reduce computational complexity and improve real-time applicability. Additionally, integrating the ANN-based MPPT algorithm with other advanced control strategies and smart grid technologies could provide new opportunities for enhancing the efficiency and resilience of renewable energy systems. In an innovative grid environment, for instance, the MPPT system could communicate with other distributed energy resources and storage systems, facilitating coordinated energy flow, adaptive control, and demand response, ultimately improving grid stability and supporting predictive maintenance for PV systems. In conclusion, the proposed ANN-based MPPT algorithm represents a significant advancement in the field of PV systems, offering higher energy yields, enhanced efficiency, and greater adaptability to dynamic environmental conditions. Its ability to outperform conventional methods, particularly under complex shading conditions, positions it as a promising candidate for future integration into next-generation RES.

REFERENCES

[1] U. Hussan, H. Wang, M. A. Ayub, H. Rasheed, M. A. Majeed, J. Peng, and H. Jiang, "Decentralized stochastic recursive gradient method for fully decentralized opf in multi-area power systems," *Mathematics*, vol. 12, no. 19, 2024. [Online]. Available: https://www.mdpi.com/2227-7390/12/19/3064

[2] M. Hamza Zafar, N. Mujeeb Khan, A. Feroz Mirza, M. Mansoor, N. Akhtar, M. Usman Qadir, N. Ali Khan, and S. K. Raza Moosavi, "A novel meta-heuristic optimization algorithm based mppt control technique for pv systems under complex partial shading condition," *Sustainable Energy Technologies and Assessments*, vol. 47, p. 101367, 2021. [Online]. Available: https://www.sciencedirect.com/science/article/pii/S2213138821003775

[3] U. Hussan, M. Hassan, M. A. Ayub, J. Peng, H. Rasheed, H. Jiang, and F. Asghar, "Smooth and uninterrupted operation of standalone dc microgrid under high and low penetration of ress," *IEEE Access*, vol. 12, pp. 48 620–48 629, 2024.

[4] M. Mao, L. Zhang, H. Huang, B. Chong, and L. Zhou, "Maximum power exploitation for grid-connected pv system under fast-varying solar irradiation levels with modified salp swarm algorithm," *Journal of Cleaner Production*, vol. 268, p. 122158, 2020. [Online]. Available: https://www.sciencedirect.com/science/article/pii/S0959652620322058

[5] S. Javed and K. Ishaque, "A comprehensive analyses with new findings of different pso variants for mppt problem under partial shading," *Ain Shams Engineering Journal*, vol. 13, no. 5, p. 101680,

This work is licensed under a Creative Commons Attribution-NonCommercial-NoDerivatives 4.0 License.
For more information, see https://creativecommons.org/licenses/by-nc-nd/4.0/

This article has been accepted for publication in IEEE Access. This is the author's version which has not been fully edited and
content may change prior to final publication. Citation information: DOI 10.1109/ACCESS.2025.3572554

2022. [Online]. Available: https://www.sciencedirect.com/science/article/pii/S2090447921004585

[6] M. Abdulkadir, A. H. M. Yatim, and S. T. Yusuf, "An improved pso-based mppt control strategy for photovoltaic systems," *International Journal of Photoenergy*, vol. 2014, no. 1, p. 818232, 2014. [Online]. Available: https://onlinelibrary.wiley.com/doi/abs/10.1155/2014/818232

[7] M. H. Qais, H. M. Hasanien, and S. Alghuwainem, "Parameters extraction of three-diode photovoltaic model using computation and harris hawks optimization," *Energy*, vol. 195, p. 117040, 2020. [Online]. Available: https://www.sciencedirect.com/science/article/pii/S036054422030147X

[8] M. Mansoor, A. F. Mirza, and Q. Ling, "Harris hawk optimization-based mppt control for pv systems under partial shading conditions," *Journal of Cleaner Production*, vol. 274, p. 122857, 2020. [Online]. Available: https://www.sciencedirect.com/science/article/pii/S0959652620329024

[9] S. Mirjalili, S. M. Mirjalili, and A. Lewis, "Grey wolf optimizer," *Advances in Engineering Software*, vol. 69, pp. 46–61, 2014. [Online]. Available: https://www.sciencedirect.com/science/article/pii/S0965997813001853

[10] S. Mohanty, B. Subudhi, and P. K. Ray, "A new mppt design using grey wolf optimization technique for photovoltaic system under partial shading conditions," *IEEE Transactions on Sustainable Energy*, vol. 7, no. 1, pp. 181–188, Jan 2016.

[11] I. S. Millah, P. C. Chang, D. F. Teshome, R. K. Subroto, K. L. Lian, and J.-F. Lin, "An enhanced grey wolf optimization algorithm for photovoltaic maximum power point tracking control under partial shading conditions," *IEEE Open Journal of the Industrial Electronics Society*, vol. 3, pp. 392–408, 2022.

[12] M. A. Ayub, U. Hussan, H. Rasheed, Y. Liu, and J. Peng, "Optimal energy management of mg for cost-effective operations and battery scheduling using bwo," *Energy Reports*, vol. 12, pp. 294–304, 2024. [Online]. Available: https://www.sciencedirect.com/science/article/pii/S2352484724003500

[13] M. T. Hussain, M. Shahabuddin, L.-Y. Huang, A. Sarwar, M. Asim, S. Ahmad, H.-D. Liu, and M. Tariq, "Enhanced mpp tracking in partial shading conditions for solar pv systems: A metaheuristic approach utilizing projectile search algorithm," *IEEE Access*, vol. 13, pp. 50 895–50 917, 2025.

[14] M. Z. Yousaf, M. A. Koondhar, Z. A. Zaki, E. M. Ahmed, Z. M. Alaas, I. Mahariq, and J. M. Guerrero, "Improved mppt of solar pv systems under different environmental conditions utilizes a novel hybrid pso," *Renewable Energy*, vol. 244, p. 122709, 2025. [Online]. Available: https://www.sciencedirect.com/science/article/pii/S0960148125003714

[15] J. Águila León, C. Vargas-Salgado, D. Díaz-Bello, and C. Montagud-Montalvá, "Optimizing photovoltaic systems: A meta-optimization approach with gwo-enhanced pso algorithm for improving mppt controllers," *Renewable Energy*, vol. 230, p. 120892, 2024. [Online]. Available: https://www.sciencedirect.com/science/article/pii/S0960148124009601

[16] H. Gundogdu, A. Demirci, S. M. Tercan, and U. Cali, "A novel improved grey wolf algorithm based global maximum power point tracker method considering partial shading," *IEEE Access*, vol. 12, pp. 6148–6159, 2024.

[17] G. Hou and Z. Guo, "Maximum power point tracking of solar photovoltaic under partial shading conditions based on improved salp swarm algorithm," *Electric Power Systems Research*, vol. 241, p. 111316, 2025. [Online]. Available: https://www.sciencedirect.com/science/article/pii/S0378779624012021

[18] K. Krishnaram, T. S. Padmanabhan, F. Alsaif, and S. Senthilkumar, "Performance optimization of interleaved boost converter with ANN supported adaptable stepped-scaled P&O based MPPT for solar powered applications," *Sci. Rep.*, vol. 14, no. 1, p. 8115, Apr. 2024.

[19] M. Mishra, P. Mahajan, and R. Garg, "Implementation and comparison of metaheuristically modified ANN MPPT controllers under varying solar irradiance conditions," *Electr. Eng. (Berl., Print)*, vol. 106, no. 3, pp. 3427–3443, Jun. 2024.

[20] S. Gul, S. M. Malik, Y. Sun, and F. Alsaif, "An artificial neural network based mppt control of modified flyback converter for pv systems in active buildings," *Energy Reports*, vol. 12, pp. 2865–2872, 2024. [Online]. Available: https://www.sciencedirect.com/science/article/pii/S2352484724005754

[21] S.-P. Ye, Y.-H. Liu, H.-Y. Pai, A. Sangwongwanich, and F. Blaabjerg, "A novel ann-based gmppt method for pv systems under complex partial shading conditions," *IEEE Transactions on Sustainable Energy*, vol. 15, no. 1, pp. 328–338, 2024.

[22] L. Liu and C. Liu, "A novel combined particle swarm optimization and genetic algorithm mppt control method for multiple photovoltaic arrays at partial shading," *Journal of Energy Resources Technology*, vol. 135, no. 1, p. 012002, 12 2012. [Online]. Available: https://doi.org/10.1115/1.4007940

[23] B. Jamali, M. Rasekh, F. Jamadi, R. Gandomkar, and F. Makiabadi, "Using pso-ga algorithm for training artificial neural network to forecast solar space heating system parameters," *Applied Thermal Engineering*, vol. 147, pp. 647–660, 2019. [Online]. Available: https://www.sciencedirect.com/science/article/pii/S1359431118343771

[24] T. Boukelia, O. Arslan, and M. Mecibah, "Ann-based optimization of a parabolic trough solar thermal power plant," *Applied Thermal Engineering*, vol. 107, pp. 1210–1218, 2016.

This work is licensed under a Creative Commons Attribution-NonCommercial-NoDerivatives 4.0 License.
For more information, see https://creativecommons.org/licenses/by-nc-nd/4.0/

This article has been accepted for publication in IEEE Access. This is the author's version which has not been fully edited and
content may change prior to final publication. Citation information: DOI 10.1109/ACCESS.2025.3572554

[Online]. Available: https://www.sciencedirect.com/science/article/pii/S1359431116312157

[25] C. G. Villegas-Mier, J. Rodriguez-Resendiz, J. M. Álvarez Alvarado, H. Rodriguez-Resendiz, A. M. Herrera-Navarro, and O. Rodríguez-Abreo, "Artificial neural networks in mppt algorithms for optimization of photovoltaic power systems: A review," *Micromachines*, vol. 12, no. 10, 2021. [Online]. Available: https://www.mdpi.com/2072-666X/12/10/1260

[26] M. J. Khan and L. Mathew, "Artificial neural network-based maximum power point tracking controller for real-time hybrid renewable energy system," *Soft Computing*, vol. 25, no. 8, pp. 6557–6575, 2021. [Online]. Available: https://doi.org/10.1007/s00500-021-05653-0

[27] K. S. Garud, S. Jayaraj, and M.-Y. Lee, "A review on modeling of solar photovoltaic systems using artificial neural networks, fuzzy logic, genetic algorithm and hybrid models," *International Journal of Energy Research*, vol. 45, no. 1, pp. 6–35, 2021. [Online]. Available: https://onlinelibrary.wiley.com/doi/abs/10.1002/er.5608

[28] I. Dagal, B. Akın, and E. Akboy, "A novel hybrid series salp particle swarm optimization (sspso) for standalone battery charging applications," *Ain Shams Engineering Journal*, vol. 13, no. 5, p. 101747, 2022. [Online]. Available: https://www.sciencedirect.com/science/article/pii/S2090447922000582

[29] I. Dagal and B. Akin, "Improved particle swarm optimization based on buck-boost converter (ipso-bbc) for photovoltaic system applications," *Recent Adv. Sci. Eng*, vol. 2, no. 2, pp. 42–48, 2022. [Online]. Available: https://rase.yildiz.edu.tr/article/7

[30] F. Salvaire, "Pyspice," n.d., accessed: 2024-08-25. [Online]. Available: https://pyspice.fabrice-salvaire.fr

[31] R. Venkateswari and N. Rajasekar, "Review on parameter estimation techniques of solar photovoltaic systems," *International Transactions on Electrical Energy Systems*, vol. 31, no. 11, p. e13113, 2021. [Online]. Available: https://onlinelibrary.wiley.com/doi/abs/10.1002/2050-7038.13113

[32] E. Batzelis, "Non-iterative methods for the extraction of the single-diode model parameters of photovoltaic modules: A review and comparative assessment," *Energies*, vol. 12, no. 3, 2019. [Online]. Available: https://www.mdpi.com/1996-1073/12/3/358

[33] B. Maniraj and A. Peer Fathima, "Parameter extraction of solar photovoltaic modules using various optimization techniques: a review," *Journal of Physics: Conference Series*, vol. 1716, no. 1, p. 012001, dec 2020. [Online]. Available: https://dx.doi.org/10.1088/1742-6596/1716/1/012001

[34] F. E. Ndi, S. N. Perabi, S. E. Ndjakomo, G. Ondoua Abessolo, and G. Mengounou Mengata, "Estimation of single-diode and two diode solar cell parameters by equilibrium optimizer method," *Energy Reports*, vol. 7, pp. 4761–4768, 2021. [Online]. Available: https://www.sciencedirect.com/science/article/pii/S235248472100490X

[35] M. H. Qais, H. M. Hasanien, and S. Alghuwainem, "Identification of electrical parameters for three-diode photovoltaic model using analytical and sunflower optimization algorithm," *Applied Energy*, vol. 250, pp. 109–117, 2019. [Online]. Available: https://www.sciencedirect.com/science/article/pii/S0306261919308682

[36] O. S. Elazab, H. M. Hasanien, I. Alsaidan, A. Y. Abdelaziz, and S. M. Muyeen, "Parameter estimation of three diode photovoltaic model using grasshopper optimization algorithm," *Energies*, vol. 13, no. 2, 2020. [Online]. Available: https://www.mdpi.com/1996-1073/13/2/497

[37] J. Bastidas-Rodriguez, G. Petrone, C. Ramos-Paja, and G. Spagnuolo, "A genetic algorithm for identifying the single diode model parameters of a photovoltaic panel," *Mathematics and Computers in Simulation*, vol. 131, pp. 38–54, 2017, 11th International Conference on Modeling and Simulation of Electric Machines, Converters and Systems. [Online]. Available: https://www.sciencedirect.com/science/article/pii/S0378475415002220

[38] T. Ikegami, T. Maezono, F. Nakanishi, Y. Yamagata, and K. Ebihara, "Estimation of equivalent circuit parameters of pv module and its application to optimal operation of pv system," *Solar Energy Materials and Solar Cells*, vol. 67, no. 1, pp. 389–395, 2001, pVSEC 11 - PART III. [Online]. Available: https://www.sciencedirect.com/science/article/pii/S092702480000307X

[39] W. De Soto, S. Klein, and W. Beckman, "Improvement and validation of a model for photovoltaic array performance," *Solar Energy*, vol. 80, no. 1, pp. 78–88, 2006. [Online]. Available: https://www.sciencedirect.com/science/article/pii/S0038092X05002410

[40] W. F. Holmgren, C. W. Hansen, and M. A. Mikofski, "pvlib python: a python package for modeling solar energy systems," *Journal of Open Source Software*, vol. 3, no. 29, p. 884, 2018, dOI: 10.21105/joss.00884. [Online]. Available: https://doi.org/10.21105/joss.00884

[41] H. Patel and V. Agarwal, "Matlab-based modeling to study the effects of partial shading on pv array characteristics," *IEEE Transactions on Energy Conversion*, vol. 23, no. 1, pp. 302–310, March 2008.

[42] J. Ahmed and Z. Salam, "An improved method to predict the position of maximum power point during partial shading for pv arrays," *IEEE Transactions on Industrial Informatics*, vol. 11, no. 6, pp. 1378–1387, Dec 2015.

[43] A. Kouchaki, H. Iman-Eini, and B. Asaei, "A new maximum power point tracking strategy for pv arrays under uniform and non-uniform insolation

This work is licensed under a Creative Commons Attribution-NonCommercial-NoDerivatives 4.0 License.
For more information, see https://creativecommons.org/licenses/by-nc-nd/4.0/

This article has been accepted for publication in IEEE Access. This is the author's version which has not been fully edited and
content may change prior to final publication. Citation information: DOI 10.1109/ACCESS.2025.3572554

conditions," *Solar Energy*, vol. 91, pp. 221–232, 2013. [Online]. Available: https://www.sciencedirect.com/science/article/pii/S0038092X13000248

[44] H. Patel and V. Agarwal, "Maximum power point tracking scheme for pv systems operating under partially shaded conditions," *IEEE Transactions on Industrial Electronics*, vol. 55, no. 4, pp. 1689–1698, April 2008.

[45] Z. Yan, X. Zhu, X. Wang, Z. Ye, F. Guo, L. Xie, and G. Zhang, "A multi-energy load prediction of a building using the multi-layer perceptron neural network method with different optimization algorithms," *Energy Exploration & Exploitation*, vol. 41, no. 1, pp. 273–305, 2023. [Online]. Available: https://doi.org/10.1177/01445987221112250

[46] K. Punitha, D. Devaraj, and S. Sakthivel, "Artificial neural network based modified incremental conductance algorithm for maximum power point tracking in photovoltaic system under partial shading conditions," *Energy*, vol. 62, pp. 330–340, 2013. [Online]. Available: https://www.sciencedirect.com/science/article/pii/S036054421300697X

[47] O. Kramer, *Scikit-Learn*. Cham: Springer International Publishing, 2016, pp. 45–53. [Online]. Available: https://doi.org/10.1007/978-3-319-33383-0_5

[48] H. Salem, A. Kabeel, E. M. El-Said, and O. M. Elzeki, "Predictive modelling for solar power-driven hybrid desalination system using artificial neural network regression with adam optimization," *Desalination*, vol. 522, p. 115411, 2022. [Online]. Available: https://www.sciencedirect.com/science/article/pii/S0011916421004823

[49] H. Gundogdu, A. Demirci, S. M. Tercan, and U. Cali, "A novel improved grey wolf algorithm based global maximum power point tracker method considering partial shading," *IEEE Access*, vol. 12, pp. 6148–6159, 2024.



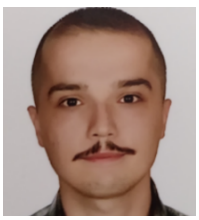
ALPASLAN DEMIRCI received the B.Sc. degree in electrical and electronics engineering from Sakarya University, Turkey, the B.Sc. and M.Sc. degrees in electrical education from Marmara University, İstanbul, Turkey, in 2007 and 2011, respectively, and the Ph.D. degree in electrical engineering from the Graduate School of Science and Engineering, Yildiz Technical University (YTU), İstanbul, in 2023. He is currently an Associate Professor with the Department of Electrical Engineering, YTU. His research interests include power system optimization methods, distributed renewable energy systems, energy economics, electric vehicles, and energy storage systems. He has published several articles related his research areas.



IDRISS DAGAL was born in Kouno, Chad, and holds a B.S. in Industrial and Maintenance Engineering from Mongo Polytechnics University, Chad (2006), an M.S. in Aeronautical Engineering from the Ethiopian Airlines School, Ethiopia (2010), and a Ph.D. in Electrical and Electronics Engineering from Yildiz Technical University, Turkey (2022). He began his career as an Aircraft Engineer at Chad's Air Force Company (2010–2012) and is currently an Assistant Professor at Istanbul Beykent University (since 2024). An accomplished researcher, he has authored over 30 publications, serves as a reviewer for top-tier journals, and has leadership training from the U.S. Department of State's African Civic Engagement Program at the University of Georgia. His expertise spans optimization algorithms, artificial intelligence (AI), Avionics, renewable energy, and power electronics, with a focus on advancing sustainable energy and intelligent systems through interdisciplinary research.



SAID MIRZA TERCAN received the B.Sc. degree from the Department of Electrical Engineering, Istanbul Technical University in 2012, the M.Sc. and Ph.D. degrees in Electrical Engineering from the Graduate School of Science and Engineering, Yıldız Technical University (YTU), in 2015 and 2022, respectively. He currently serves an Assistant Professor at the Department of Electrical Engineering, YTU. His research interests are energy storage systems, power distribution grid, renewable energy systems, electric vehicles. He has published several articles and conference papers related his research areas.



MUSA TERKES received the B.Sc. degree in electrical engineering from Yildiz Technical University (YTU), Istanbul, Türkiye, in 2019, and the M.Sc. degree in electrical power systems from Graduate School of Science and Engineering, YTU, in 2022. He has been studying for a PhD in Electrical Power Systems from the Graduate School of Science and Engineering at YTU since 2023. He assists in power systems, fault analysis, energy transmission, and distribution systems course and teaches electrical power systems, lighting, electrical internal installation, and high voltage laboratories. His research interests include optimal sizing of hybrid power systems, control methods for energy storage systems, energy economics, benefits of renewable energy systems, grid effects of electric vehicles, energy management allocation of microgrids, second-life battery feasibility, and aging. He has published several articles related his research areas.

This work is licensed under a Creative Commons Attribution-NonCommercial-NoDerivatives 4.0 License.
For more information, see https://creativecommons.org/licenses/by-nc-nd/4.0/

This article has been accepted for publication in IEEE Access. This is the author's version which has not been fully edited and content may change prior to final publication. Citation information: DOI 10.1109/ACCESS.2025.3572554



HASAN GUNDOGDU received the B.Sc. degree in Electrical Engineering from Yildiz Technical University, Istanbul, Turkey in 2021. He continues his education in M.Sc. Degree on Electrical Machines and Power Electronics in Yildiz Technical University. Since 2021, he has been working as an electrical engineer in Propulsion Electronic System Team. His research interest includes renewable energy system, electrical machines, power electronics, UAVs and electrical vehicles. He published several papers related his research areas.



UMIT CALI earned his B.E. degree in Electrical Engineering from Yildiz Technical University, Istanbul, Turkey in 2000, and his M.Sc. degree in Electrical Communication Engineering and Ph.D. degree in Electrical Engineering and Computer Science from the University of Kassel, Germany, in 2005 and 2010, respectively. With over 20 years of experience in both industry and academia, he currently serves as a Professor of Digital Engineering for Future Technologies at the University of York. His research interests encompass energy informatics, artificial intelligence, blockchain technology, renewable energy systems, and energy economics. He holds the position of Chair for the Digital Privacy-Energy Industry TC under IEEE Future Directions and serves as Vice Chair for the IEEE Blockchain in Energy Standards WG (P2418.5).

This work is licensed under a Creative Commons Attribution-NonCommercial-NoDerivatives 4.0 License.
For more information, see https://creativecommons.org/licenses/by-nc-nd/4.0/